

正確な転移部位の同定には、ex vivoへの摘出臓器単位での評価が必要であった。

D. 考察

T細胞やB細胞等の重要な免疫担当細胞を欠落した重症免疫不全マウスは開腹手術や心室穿刺等の外科学的侵襲に必ずしも敏感ではない。このことは、SCIDマウス及びNOD/SCIDマウスを用いる小動物実験がヒトがん細胞に対する重要な動物資源として利用できることを示唆している。すなわち、異種移植実験であり、必ずしも完全な免疫系をもたない動物資源ではあるが、ヒトがん細胞を標的とした分子標的薬等の創薬開発試験ではin vitro から動物実験 (in vivo) まで共通した評価系を与えることを示唆している。

本研究によりルシフェラーゼ発現ヒトがん細胞株の発光量は細胞株に依存することが示された。このことは細胞の分化状態と相関する傾向にあり、特に高分化型腺癌では著しく発光量が減弱する傾向にあった。遺伝子導入後の選択薬剤はピューロマシンをを用いているが、単純にこれらががん細胞株が遺伝子導入ベクター非依存的にピューロマシンの耐性を獲得している可能性も否定できず、細胞の分化状態、もしくはがん細胞に固有の薬剤耐性遺伝子の発動によるものであるのかなど、今後の検討課題としたい。

これまでに作製したヒトがん細胞株ルミネッセンス発光量とマウス個体内検出限界を評価した結果、50,000単位 ($/10^5$ 個) 以上の発光量が必要であることが示唆された。このことは、今後作製されるべき細胞の発光量の基準として利用することができる。がん幹細胞研究では、NOD/SCIDマウスへの移植細胞数が幹細胞分画を含むもので 10^2 個 - 10^3 個レベルであるため、幹細胞研究への応用の観点から100,000単位 ($/10^5$ 個) 以上の検出感度を持つ細胞株の作製を目標としたい。

また、移植癌の進展による腫瘍増大は非常に強い発光をもたらし、微少多臓器転移巢の描出に対して欠点をもたらした。このことは、白毛マウスにおいて発光が散乱する傾向にあった。現行の高感度CCDカメラや機器の検出感度が自動調節されているためであり、閾値設定等のモード調節機構が搭載されることが望ましい。したがって、光学機器メーカーとの産学協力によりこの問題点を解決する必要がある。併せて通常のBalb/cヌードマウスよりも免疫不全型のヘアレスマウスのイメージング専用の動物資源開発も重要な案件と考えられた。

E. 結論

SCIDマウス及びNOD/SCIDマウスは外科学的侵襲に耐性であり、ヒトがん細胞を標的とした創薬開発試験ではin vitro から動物実験 (in vivo) まで共通した評価系として利用可能である。しかしながら、ルミネッセンス発光のマウスイメージング解析には観察期間中決まったポジションを定める必要がある。

F. 健康危険情報

該当なし (省略)

G. 研究発表

1. 論文発表

1. Yanagisawa S, Kadouchi I, Yokomori K, Hirose M, Hakozaiki M, Hojo H, Maeda K, Kobayashi E, Murakami T. Identification and metastatic potential of tumor-initiating cells in malignant rhabdoid tumor of the kidney. *Clin Cancer Res*. 2009, in press.
2. Horie M, Sekiya I, Muneta T, Ichinose S, Matsumoto K, Saito H, Murakami T, Kobayashi E. Intra-articular injected synovial stem cells

- differentiate into meniscal cells directly and promote meniscal regen-eration without mobilization to distant organs in rat massive meniscal defect. **Stem Cells** 2009, in press.
3. Endo T, Ajiki T, Inoue H, Kikuchi M, Yashiro T, Nakama T, Hoshino Y, Murakami T, Kobayashi E. Implication of a neuropathic pain by enforced stepping exercise with aberrant axonal sprouting through brain-derived neurotrophic factor. **Biochem Biophys Res Commun**. 2009, in press.
 4. Mato N, Fujii M, Hakamata Y, Kobayashi E, Sato A, Hayakawa M, Ohto-Ozaki H, Bando M, Ohno S, Tominaga S, Sugiyama Y. IL-1R-related protein ST2 suppressed the initial stage of bleomycin-induced lung injury. **Eur Respir J**. 2009, in press.
 5. Madoiwa S, Yamauchi T, Kobayashi E, Hakamat-a Y, Dokai M, Makino N, Kashiwakura Y, Ishiwata A, Ohmori T, Mimuro J, Sakata Y. Induction of factor VIII-specific unresponsiveness by intrathymic factor VIII injection in murine hemophilia A. **J Thromb Haemost**. 2009, in press.
 6. Arao Y, Hakamata Y, Igarashi Y, Sato Y, Kayama Y, Takahashi M, Kobayashi E, Murakami T. Characterization of hepatic sexual dimorphism in Alb-DsRed2 transgenic rats. **Biochem Biophys Res Commun**. 2009, in press.
 7. Kadouchi I, Sakamoto K, Tangjiao L, Murakami T, Kobayashi E, Hoshino Y, Yamaguchi Y. Latexin is involed in bone morphogentic protein-2-induced chondrocyte differentiation. **Biochem. Biophys. Res. Commun**. 2009 Jan 16; 378(3): 600-604.
 8. Inoue H, Murakami T, Ajiki T, Hara M, Hoshino Y, Kobayashi E. Bioimaging assessment and effect of skin wound healing using bone-marrow-derived mesenchymal stromal cells with the artificial dermis in diabetic rats. **J Biomed Opt**. 2008; 13 (6): 064036(1-10).
 9. Murakami T, Sato A, Chun NAL, Hara M, Naito Y, Kobayashi Y, Kano Y, Ohtsuki M, Furukawa Y, Kobayashi E. Transcriptional Modulation Using HDACi Depsipeptide Promotes Immune Cell-Mediated Tumor Destruction of Murine B16 Melanoma. **J Invest Dermatol**. 2008; 128: 1506-1516.
 10. Hara M, Murakami T, Kobayashi E. In vivo bioimaging using photogenic rats: Fate of ingected bone marrow derived mesenchymal atromal cells. **J Autoimm**. 2008; 30 (3): 163-171.
 11. Yokoo T, Fukui A, Matsumoto K, Ohashi T, Sado, Y, Suzuki H, Kawamura T, Okabe M, Hosoya T, Kobayashi E. Generation of a Transplantable Erythropoietin-Producer Derived From Human Mesenchymal Stem Cells. **Transplantation**. 85 (11): 1654-1658, 2008.
 12. 村上 孝、小林英司: 「ラット」を基盤とした In vivo バイオイメージング. 実験医学2008; 26(17):110-117.
 13. 村上 孝、小林英司: 臓器組織再生を目指した細胞・幹細胞移植研究の動向. 今日の移植 2008; 21 (4): 313-318.
 14. 小林英司、村上 孝: 再生医療研究用幹細胞や癌細胞の動態観察に貢献する『color-engineered』ラットシステム. BIO EX-press 新緑号: 34-39, 2008.
 15. 井上泰一、安食孝士、遠藤照顕、中間季雄、星野雄一、村上 孝、小林英司: トランスジェニックラットを用いた移植骨髄由来細胞のバイオイメージング. 日本整形外科学会誌 82: 983-988, 2008.
2. 学会発表
 1. Kai K, Teraoka S, Adachi Y, Ikehara S,

- Murakami T, Kobayashi E. In vivo cell kinetics of bone marrow transplantation using dual colored transgenic rat system. Jan. 21-22, 2008. San Jose, CA, USA.
2. Horie M, Sekiya I, Muneta T, Murakami T, Kobayashi E. Establishment of mesenchymal stem cells derived from bone marrow and synovium of transgenic rats expressing dual reporter genes. Jan. 21-22, 2008. San Jose, CA, USA.
3. Kikuchi T, Hotta J, Murakami T, Kobayashi E. A Novel Visualization System of Organ/Tissue ATP Levels Using Luciferase Transgenic Rats. American Transplant Congress 2008; May 30-June 4, 2008. Toronto, Canada.
4. 小林英司: 臓器保存液開発における画期的システム—Luciferase Transgenic ラットを用いたスクリーニング法— シンポジウム「臓器移植関連の生体イメージング」第35回日本臓器保存生物医学会定期学術集会 2008年11月23日東京.
5. 村上孝, 小林英司: ラット生体内イメージングがもたらす臓器移植研究の進歩 シンポジウム「臓器移植関連の生体イメージング」第35回日本臓器保存生物医学会定期学術集会 2008年11月23日東京.
- H. 知的財産権の出願・登録状況（予定を含む。）
1. 特許取得
 5. 幹細胞の分化能の評価方法（出願）
 6. 凍結保存臓器を用いた腎生検シュミレーションキット（出願）
 7. 食品保存方法の評価方法（出願）
 8. 人工臓器前駆体およびその製造方法（出願）
 2. 実用新案登録
該当なし
 3. その他
該当なし

研究成果の刊行に関する一覧表

雑誌

発表者氏名	論文タイトル名	発表誌名	巻号	ページ	出版年
Yanagisawa S, Kadouchi I, Yokomori K, Hirose M, Hakozaki M, Hojo H, Maeda K, <u>Kobayashi E</u> , <u>Murakami T</u> .	Identification and metastatic potential of tumor-initiating cells in malignant rhabdoid tumor of the kidney.	<i>Clin Cancer Res.</i>	In press		2009
Horie M, Sekiya I, Muneta T, Ichinose S, Matsumoto K, Saito H, <u>Murakami T</u> , <u>Kobayashi E</u> .	Intraarticular injected synovial stem cells differentiate into meniscal cells directly and promote meniscal regeneration without mobilization to distant organs in rat massive meniscal defect.	<i>Stem Cells</i>	In press		2009
Endo T, Ajiki T, Inoue H, Kikuchi M, Yashiro T, Nakama T, Hoshino Y, <u>MURAKAMI T</u> , <u>Kobayashi E</u> .	Implication of a neuropathic pain by enforced stepping exercise with aberrant axonal sprouting through brain-derived neurotrophic factor.	<i>Biochem Biophys Res Commun.</i>	In press		2009
Mato N, Fujii M, Hakamata Y, <u>Kobayashi E</u> , Sato A, Hayakawa M, Ohto-Ozaki H, Bando M, Ohno S, Tominaga S, Sugiyama Y.	IL-1R-related protein ST2 suppressed the initial stage of bleomycin-induced lung injury.	<i>Eur Respir J</i>	In press		2009
Madoiwa S, Yamauchi T, <u>Kobayashi E</u> , Hakamat-a Y, Dokai M, Makino N, Kashiwakura Y, Ishiwata A, Ohmori T, Mimuro J, Sakata Y.	Induction of factor VIII-specific unresponsiveness by intrathymic factor VIII injection in murine hemophilia A.	<i>J Thromb Haemost</i>	In press		2009

Arao Y, Hakamata Y, Igarashi Y, Sato Y, Kayama Y, Takahashi M, <u>Kobayashi E</u> , <u>Murakami T</u> .	Characterization of hepatic sexual dimorphism in Alb-DsRed2 transgenic rats.	<i>Biochem Biophys Res Commun.</i>	In press		2009
Kadouchi I, Sakamoto K, Tangjiao L, <u>Murakami T</u> , <u>Kobayashi E</u> , Hoshino Y, Yamaguchi Y.	Latexin is involved in bone morphogenetic protein-2-induced chondrocyte differentiation.	<i>Biochem. Biophys. Res. Commun.</i>	378(3)	600-604	2009
Inoue H, <u>Murakami T</u> , Ajiki T, Hara M, Hoshino Y, <u>Kobayashi E</u> .	Bioimaging assessment and effect of skin wound healing using bone marrow-derived mesenchymal stromal cells with the artificial dermis in diabetic rats.	<i>Journal of Biomedical Optics.</i>	13(6)	064036	2008
<u>Murakami T</u> , Sato A, Chun NAL, Hara M, Naito Y, Kobayashi Y, Kano Y, Furukawa Y, <u>Kobayashi E</u> .	Transcriptional modulation using HDACi depsipeptide promotes immune cell-mediated tumor destruction of murine B16 melanoma.	<i>J Invest Dermatol</i>	28(6)	1506-1516	2008
Hara M, <u>Murakami T</u> , <u>Kobayashi E</u> .	<i>In vivo</i> bioimaging using photogenic rats: fate of injected bone marrow-derived mesenchymal stromal cells.	<i>J Autoimmun</i>	30	163-171	2008
<u>村上 孝</u> , <u>小林英司</u>	「ラット」を基盤とした In vivo バイオイメージング。	実験医学	26(17)	110-117	2008
<u>村上 孝</u> , <u>小林英司</u>	臓器組織再生を目指した細胞・幹細胞移植研究の動向	今日の移植	21 (4)	313-318	2008
<u>村上 孝</u> , <u>小林英司</u>	蛍光発生トランスジェニックラットがもたらすイノベーション。	日本コンピュータ外科学会誌	10 (4)	495-499	2008
<u>小林英司</u> , <u>村上 孝</u>	再生医療研究用幹細胞や癌細胞の動態観察に貢献する『color-engineered』ラットシステム。	BIO EX-press	新緑号	34-39	2008

井上泰一、 安食孝士、 遠藤照顕、 中間季雄、 星野雄一、 村上 孝、 小林英司	トランスジェニックラットを用いた移植骨髄由来細胞のバイオイメージング。	日本整形外科学会誌	82	983-988	2008
--	-------------------------------------	-----------	----	---------	------

Transcriptional Modulation Using HDACi Depsipeptide Promotes Immune Cell-Mediated Tumor Destruction of Murine B16 Melanoma

Takashi Murakami¹, Atsuko Sato^{1,2}, Nicole A.L. Chun¹, Mayumi Hara¹, Yuki Naito¹, Yukiko Kobayashi^{2,3}, Yasuhiko Kano⁴, Mamitaro Ohtsuki², Yusuke Furukawa³ and Eiji Kobayashi¹

With melanoma, as with many other malignancies, aberrant transcriptional repression is a hallmark of refractory cancer. To restore gene expression, use of a histone deacetylase inhibitor (HDACi) is expected to be effective. Our recent DNA micro-array analysis showed that the HDACi depsipeptide (FK228) significantly enhances gp100 antigen expression. Herein, we demonstrate that depsipeptide promotes tumor-specific T-cell-mediated killing of B16/F10 murine melanoma cells. First, by a quantitative assay of caspase-3/7 activity, a sublethal dose of depsipeptide was determined (ED50: 5 nM), in which p21^{Waf1/Cip1} and Fas were sufficiently evoked concomitantly with histone H3 acetylation. Second, the sublethal dose of depsipeptide treatment with either a recombinant Fas ligand or tumor-specific T cells synergistically enhanced apoptotic cell death in B16/F10 cells *in vitro*. Furthermore, we found that depsipeptide increased levels of perforin in T cells. Finally, *in vivo* metastatic growth of B16/F10 in the lung was significantly inhibited by a combination of depsipeptide treatment and immune cell adoptive transfer from immunized mice using irradiated B16 cells and gp100-specific (Pmel-1) TCR transgenic mice ($P < 0.05$, vs cell transfer alone). Consequently, employment of a transcriptional modulation strategy using HDACis might prove to be a useful pretreatment for human melanoma immunotherapy.

Journal of Investigative Dermatology (2008) **128**, 1506–1516; doi:10.1038/sj.jid.5701216; published online 10 January 2008

INTRODUCTION

Great efforts have been made in the field of tumor immunology, and attempts to enhance cellular immune responses have used various cancer antigens and immunizing vectors (Rosenberg, 2004; Gattinoni *et al.*, 2006). Although these strategies allow for the generation of immune T cells that recognize antigenic peptides present on tumor cells, the regression of growing tumors in patients treated with active immunization has been sporadic and rare (Rosenberg *et al.*, 2004). In fact, a variety of factors that limit tumor regression despite the *in vivo* generation of antitumor T cells have been reported (Rosenberg and Dudley, 2004), and it is therefore necessary to overcome many tumor and lymphocyte factors

that cause the tumor-escape mechanisms. Targeting key survival pathways in tumor cells, particularly those that allow cancer cells to prevent host immune attacks, is an attractive approach when aiming for an increase in the effectiveness of cancer immunotherapy.

There are emerging data suggesting that aberrant transcriptional repression of genes to control cell growth and differentiation is a hallmark of malignancy (Herman and Baylin, 2003). With melanoma, as with many other cancers, alteration of histone deacetylases (HDACs) underlies the transcriptional repression (Klisovic *et al.*, 2003; Kobayashi *et al.*, 2006). Thus, blockade of HDACs might restore global gene expression in cancer cells, making them sensitive to cell cycle arrest, differentiation, and apoptotic cell death (Johnstone and Licht, 2003; Minucci and Pelicci, 2006). The action mode of histone deacetylase inhibitors (HDACis), as the transcriptional modulator, differs from that of other anti-cancer agents (Marks *et al.*, 2001), and HDACis are expected to be effective for many cancer types that resist conventional chemotherapy (Marks *et al.*, 2001; Minucci and Pelicci, 2006). Indeed, HDACis have shown cytotoxicity in a variety of human and rodent cancer cells *in vitro* and *in vivo* (Hoshikawa *et al.*, 1994), some of which are being tested in clinical studies (Minucci and Pelicci, 2006).

Depsipeptide (also referred to as FK228 and FR901228) may be considered a promising HDACi for human melanoma. It was originally isolated from *Chromobacterium violaceum* (no. 968) as a compound that reversed the

¹Division of Organ Replacement Research, Center for Molecular Medicine, Jichi Medical University, Shimotuke, Tochigi, Japan; ²Department of Dermatology, Jichi Medical University, Shimotuke, Tochigi, Japan; ³Division of Stem Cell Regulation, Center for Molecular Medicine, Jichi Medical University, Shimotuke, Tochigi, Japan and ⁴Division of Medical Oncology, Tochigi Cancer Center, Utsunomiya, Tochigi, Japan

Correspondence: Dr Takashi Murakami, Division of Organ Replacement Research, Center for Molecular Medicine, Jichi Medical University, 3311-1 Yakushiji, Shimotuke, Tochigi 329-0498, Japan.
E-mail: takmu@jichi.ac.jp

Abbreviations: CTL, cytotoxic T lymphocyte; FasL, Fas ligand; FCS, fetal calf serum; HDAC, histone deacetylase; HDACi, histone deacetylase inhibitor; MHC, major histocompatibility complex; PE, phycoerythrin; RT-PCR, reverse transcription-PCR; s.c., subcutaneous

Received 7 May 2007; revised 14 September 2007; accepted 3 November 2007; published online 10 January 2008

malignant phenotype of H-ras-transformed fibroblasts by blocking the p21^{ras}-mediated signal transduction pathway (Ueda *et al.*, 1994a,b). Depsipeptide suppressed cell proliferation and induced apoptosis in human uveal melanoma cell lines at relatively high doses (Klisovic *et al.*, 2003) and produced substantial therapeutic effects on various malignancies (Minucci and Pellicci, 2006). In our previous study to determine the molecular basis of its cytotoxic effect, depsipeptide suppressed the Ras-mitogen-activated protein kinase signaling pathway through Rap1 upregulation, leading to apoptosis in human melanoma cells (Kobayashi *et al.*, 2006). Herein, we show that depsipeptide sensitized poorly immunogenic murine B16 melanoma cells to the Fas ligand and that a limited dose of depsipeptide suppressed *in vivo* growth of B16/F10 in combination with adoptive immune cell transfer therapy. Consequently, a transcriptional modulation strategy using HDACis might prove to be a useful adjunct in human immunotherapy strategies against cancer.

RESULTS

Depsipeptide enhances expression of gp100/pmel17 melanoma antigen in melanoma cell lines

Our recent DNA micro-array study revealed that the HDACi depsipeptide markedly enhanced mRNA expression of gp100/pmel17 melanoma antigen in MM-LH human melanoma cells (15-fold increase) (Kobayashi *et al.*, 2006). Thus, we initially hypothesized that gp100/pmel17 would be a potential target of depsipeptide in human melanoma cells. The expression of gp100/pmel17 in human melanoma cell lines was examined

by reverse transcription-PCR (RT-PCR) (Figure 1a). All melanoma cell lines examined showed strong enhancement of gp100/pmel17 mRNA expression after exposure to depsipeptide (10 nM) for 16 hours, whereas normal healthy melanocytes were not affected by the same dose of depsipeptide. The expression of gp100/pmel17 by depsipeptide was moderately enhanced in murine B16/F10 melanoma cells.

To characterize the effects of depsipeptide in a murine model of melanoma, we examined the ability of depsipeptide to induce histone acetylation in B16/F10 cells (Figure 1b). Basal acetylation of histone H3 (lysine residue 9) was detected, and subsequent experiments revealed that the acetylation level of histone H3 (lysine residues 9 and 18) increased significantly after a 24 hour exposure to 1–10 nM depsipeptide. Furthermore, major histocompatibility complex (MHC) class I (H2-D^b) and Fas (CD95) death receptor expression were enhanced in B16/F10 cells exposed to depsipeptide (Figure 1c). In human melanoma cell lines, to depsipeptide resulted in moderately enhanced MHC class I expression but not Fas expression (Figure S1). Thus, a 1–10 nM depsipeptide dose could sufficiently modulate murine B16/F10 melanoma cells within 16 hours *in vitro*, suggesting that a limited dose of depsipeptide may be effective for recognition and sensitization of immune cell-mediated tumor destruction in mice.

A limited dose of depsipeptide moderately induces apoptosis and cell cycle arrest in murine B16 melanoma cells

We have shown previously that depsipeptide induces apoptotic cell death in human melanoma cell lines (Kobayashi

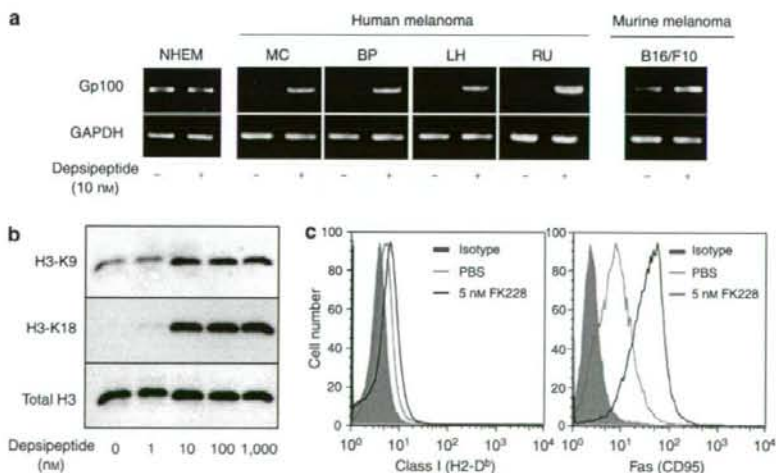


Figure 1. Depsipeptide enhances expression of gp100/pmel17 melanoma antigen. (a) RT-PCR analysis of gp100/pmel17 transcript. Total RNA was extracted from each melanoma cell line after exposure to depsipeptide (10 nM) for 16 hours. PCR was performed with primers as described in Materials and Methods. GAPDH, glyceraldehyde-3-phosphate dehydrogenase (as an internal control); NHEM, normal healthy melanocytes; MC (RPM-MC), BP (MM-BP), LH (MM-LH), and RU (MM-RU) are human melanoma cell lines. One of three independent experiments with similar results is shown. (b) Effect of depsipeptide on histone deacetylation in B16/F10 cells. B16/F10 cells (2×10^6) were exposed to depsipeptide at the indicated concentration for 16 hours. Cells were lysed and analyzed for anti-acetyl-histone H3 (Lys 9), anti-acetyl-histone H3 (Lys 18) and anti-histone H3 by western blotting. (c) Expression of MHC class I (H2-D^b) and Fas (CD95) in B16/F10 cells following exposure to depsipeptide. B16/F10 cells were exposed to depsipeptide at the indicated concentration for 16 hours and stained with PE-conjugated anti-H2D^b or Fas mAb. The control was treated with PBS. One of 2–3 independent experiments with similar results is shown.

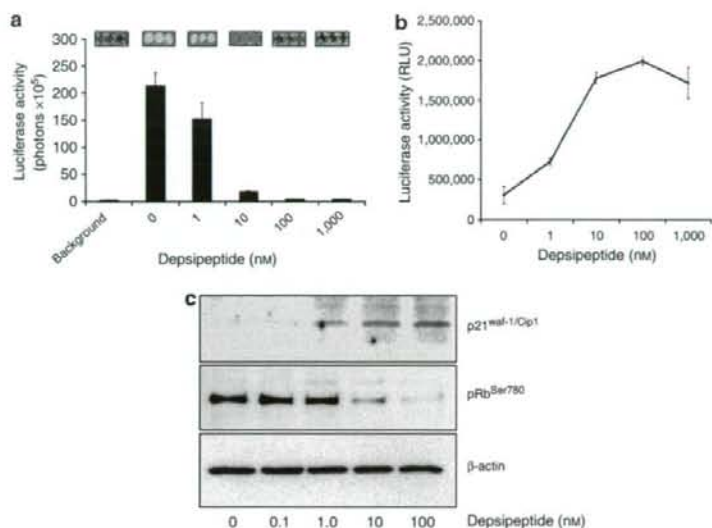


Figure 2. Depsipeptide activates caspase-3/7 and accompanies cell cycle arrest in B16/F10 cells. (a) Luc-B16/F10 cells (1×10^5) were plated onto 48-well plates at the indicated number and exposed to depsipeptide at the indicated concentration for 16 hours. Luciferase activity (photon counts) was then evaluated in the presence of D-luciferin. (b) Caspase-3/7 activity was quantified for 16 hours following treatment at the indicated concentration of depsipeptide in B16/F10 cells (2×10^4). The Caspase-Glo 3/7 Assay system (Promega) was used according to the manufacturer's instructions. The background luminescence associated with the cell culture and assay reagent (blank reaction) was subtracted from experimental values. (c) Western blot analysis of p21^{Waf1/Cip1} and phospho-RB (Ser780) 16 hours following treatment at the indicated concentration of depsipeptide. β-actin was used as an internal control. One of two independent experiments with similar results is shown.

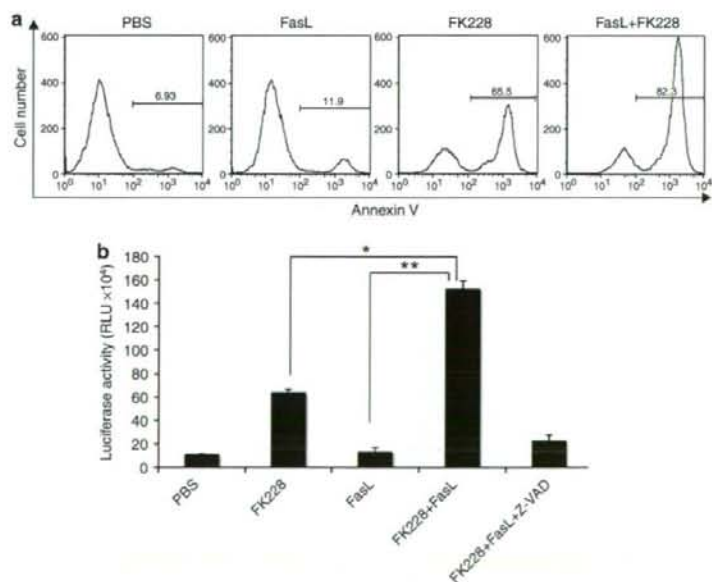


Figure 3. A sublethal dose of depsipeptide with Fas engagement synergistically promotes apoptotic cell death in B16/F10 cells *in vitro*. (a) B16/F10 cells (1×10^6) were treated with depsipeptide (5 nM) and recombinant FLAG-tagged FasL (10 ng ml^{-1}) and multimerized with anti-FLAG M2 antibodies (1 mg ml^{-1}) for 16 hours. Cells were then collected and stained with annexin-V-FITC. One of two independent experiments with similar results is shown. (b) Caspase-3/7 activity after exposure to depsipeptide with Fas engagement. The Caspase-Glo 3/7 Assay system (Promega) was used as described above. * $P < 0.05$; ** $P < 0.001$ (Student's *t*-test).

et al., 2006). As photon emission from luciferase-expressing luc-B16/F10 cells was highly correlated with viable cell number (Sato et al., 2006), we examined a sublethal dose of depsipeptide on murine B16/F10 melanoma cells (Figure 2a). Results revealed that depsipeptide decreased tumor-derived photons in a dose-dependent manner. Furthermore, caspase-3/7 activity in unmanipulated B16/F10 cells also increased linearly after a 24 hour exposure to 1–10 nM depsipeptide (Figure 2b), with the median dose of depsipeptide (ED₅₀) being 5.34 nM. The increase in caspase-3/7 activity was accompanied by a dose-dependent increase in the expression of the cell cycle regulator p21^{Waf/Cip1}, and the Rb protein was dephosphorylated at the critical residue Ser⁷⁸⁰ for the cell cycle (Figure 2c). Thus, a sublethal dose of depsipeptide could moderately induce apoptosis and cell cycle arrest in murine B16/F10 melanoma cells.

Depsipeptide with Fas death receptor engagement synergistically promotes apoptosis in B16/F10 melanoma cells

In mechanisms associated with lymphocyte-mediated tumor killing, the Fas and Fas ligand (FasL) system is a well-known major pathway in mice (Kagi et al., 1994; Caldwell et al., 2003; Lee et al., 2006). We therefore examined whether a sublethal dose of depsipeptide (ED₅₀: 5 nM) promoted FasL-triggered apoptosis. B16/F10 cells were exposed to depsipeptide in the presence or absence of multimerized FasL, which was measured by annexin-V staining (Figure 3a). In the presence of depsipeptide, B16/F10 cells readily induced apoptotic cell death after Fas–FasL crosslinking, whereas B16/F10 cells were resistant to apoptosis with Fas crosslinking alone. Caspase-3/7 activity was also synergistically enhanced in the presence of depsipeptide and FasL (Figure 3b). Pan-caspase inhibition in tumor cells treated with Z-VAD-fmk almost totally cancelled the enhanced cytotoxic effect.

We next investigated whether a sublethal dose of depsipeptide promoted cytotoxicity induced by melanoma antigen-specific cytotoxic T lymphocytes (CTLs). To generate B16/F10-specific CTLs, C57BL/6 mice were immunized twice by subcutaneous (s.c.) injection of irradiated IL-12/IL-18-transduced B16/F10 cells (Sato et al., 2006). Spleen cells from immunized mice showed enhanced production of IFN- γ (Figure 4a) and moderate killing activity with respect to B16/F10 cells (data not shown). Strikingly, the spleen cells demonstrated efficient killing of luc-B16/F10 cells in the presence of depsipeptide (Figure 4b). Furthermore, we investigated whether depsipeptide-exposed luc-B16/F10 cells could be killed by CD8⁺ T cells from a transgenic mouse (Pmel-1), which expressed V α 2V β 13 TCR from H-2D^b-restricted murine gp100-specific clone no. 9 T cells (Overwijk et al., 2003). As shown in Figure 5a, Pmel-1 T cells were also capable of efficiently killing depsipeptide-exposed luc-B16/F10 cells. Depsipeptide at 5 nM moderately enhanced the surface expression of FasL in antigen-activated Pmel-1 T cells (Figure 5b). Furthermore, to examine whether pmel-1 CTL killing of luc-B16/F10 was primarily mediated by Fas–FasL-dependent pathway, we assessed the effect of anti-FasL neutralizing antibodies on the luc-B16/F10 killing. Anti-FasL mAb (20 μ g ml⁻¹) inhibited Pmel-mediated killing of

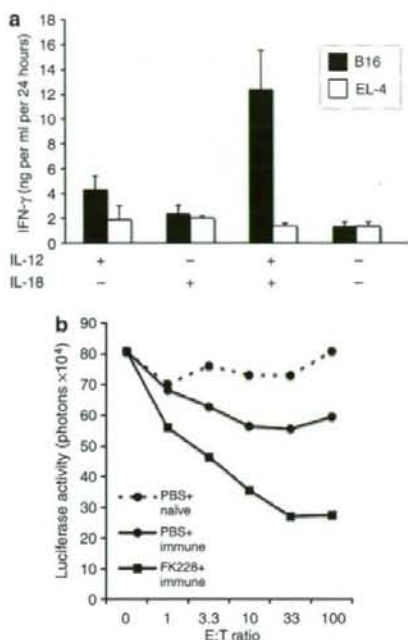


Figure 4. Melanoma-specific CTLs with depsipeptide can synergistically kill B16/F10 cells *in vitro*. (a) IFN- γ levels from splenocytes were assayed by ELISA. Splenocytes (2×10^5) were isolated after the second immunization using irradiated IL-12/IL-18 cDNA-transduced B16/F10 cells and were co-cultured for 24 hours with 1×10^5 target cells (irradiated with 80 Gy). The IFN- γ concentration of the supernatants was measured using a mouse IFN- γ immunoassay kit (R&D Systems, Minneapolis, MN) according to the manufacturer's instructions. EL-4 thymoma cells were used for control H-2^b tumor cells for a B16-specific IFN- γ increase. Error bar, SD ($n = 3$). A representative result of three independent experiments with similar results is shown. (b) Cytotoxic assay against depsipeptide-exposed luc-B16/F10 cells. C57BL/6 mice were immunized by s.c. injection of irradiated IL-12/IL-18 cDNA-transduced B16/F10 cells. Spleen cells were isolated and used as effectors at the indicated effector-to-target (E:T) ratios. Photons represent cell viability from luc-B16/F10 cells 10 hours following incubation with effector lymphocytes. Data are shown as the average of triplicate assays.

depsipeptide-treated luc-B16/F10 cells at lower effector-to-target ratios (Figure 5c). This anti-FasL mAb could not sufficiently block the Pmel-mediated killing even at a high concentration (50 μ g ml⁻¹, Figure 5d). Thus, in regard to the mechanism underlying the synergistic effect of depsipeptide and CTL cells, the CTL-mediated killing of B16 cells was not completely dependent on Fas–FasL interactions.

Depsipeptide increases perforin in activated CD8⁺ T lymphocytes

We further addressed the effects of depsipeptide on activated CD8⁺ T cells *in vitro*. The trypan blue exclusion test showed that depsipeptide at 5 nM had little effect on viability of antigen-activated Pmel-1 CTLs within 24 hours (data not shown). An alternative hypothesis is that depsipeptide may enhance immune effector cell function to produce the

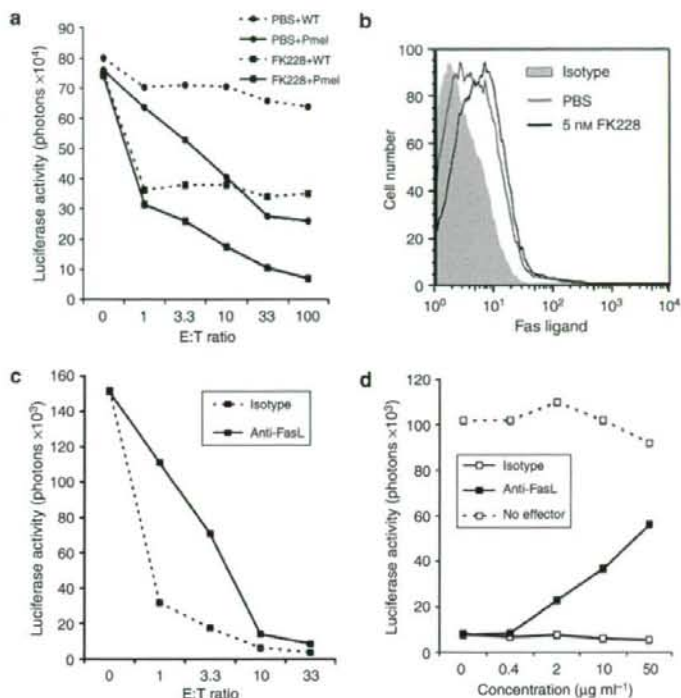


Figure 5. Gp100-specific CTLs with depsipeptide can synergistically kill B16/F10 cells *in vitro*. (a) Killing of depsipeptide-exposed luciferase-exposed B16/F10 cells by gp100-specific CD8⁺ T cells from a transgenic mouse (Pmel-1). Pmel-1 cells were used as effectors at the indicated effector-to-target (E:T) ratios. One of three independent experiments with similar results is shown. (b) Expression of FasL (CD178) in Pmel-1 T cells following exposure to depsipeptide. Antigen-stimulated Pmel-1 T cells were exposed to depsipeptide at 5 nM for 16 hours and stained with PE-conjugated anti-FasL mAb. (c) Effect of neutralizing anti-FasL mAb on Pmel-1 CTL-mediated B16/F10 killing. Depsipeptide (5 nM)-exposed luciferase-exposed B16/F10 cells were co-cultured with Pmel-1 CTLs for 16 hours in the presence of anti-FasL mAb (20 μg ml⁻¹) or isotype-matched control Ab (20 μg ml⁻¹). (d) Depsipeptide (5 nM)-exposed luciferase-exposed B16/F10 cells were incubated with Pmel-1 CTLs at a 10:1 (E:T) ratio for 16 hours with various concentrations of anti-FasL mAb. One of two independent experiments with similar results is shown.

antitumor response. Pmel-1 T cells were exposed to depsipeptide in the presence or absence of antigen stimulation, and expression of perforin was analyzed using flow cytometry (Figure 6a). Although perforin expression levels did not alter in unstimulated Pmel-1 T cells following exposure to 5 nM depsipeptide for 24 hours, cells that express perforin increased in antigen-stimulated Pmel-1 T cells. To address whether perforin mRNA expression in Pmel-1 T cells could be altered by exposure to depsipeptide, RT-PCR analysis was performed (Figure 6b). The results demonstrated that levels of perforin mRNA did not alter following exposure to multiple concentrations of depsipeptide. These results, therefore, suggest that perforin expression by exposure to depsipeptide is regulated at post-transcriptional levels. An increase of perforin was also observed in healthy human peripheral CD8⁺ T cells stimulated with phytohemagglutinin-P (PHA-P) for 24 hours (Figure 6c) and an accumulation of perforin was observed in a small number of these T cells (Figure S2). These results suggest that depsipeptide potentially increases the number of cells that express perforin in murine-activated

CD8⁺ T cells and that it enhances intracellular perforin accumulation in human T cells. These results may support the notion of an antitumor response in the host.

Inhibition of tumor growth of B16/F10 by a combination of depsipeptide with immune cell adoptive transfer therapy

To examine whether a sublethal dose of depsipeptide sensitizes B16/F10 cells *in vivo* for adoptive immunotherapy, growth retardation of established B16/F10 s.c. tumor in C57BL/6 mice (see Materials and Methods) was monitored after intraperitoneal injection of depsipeptide and subsequent adoptive transfer of Pmel-1 CTLs (Figure 7a). Depsipeptide intraperitoneal administration was performed for 3 days at the indicated doses. Established B16/F10 s.c. tumor growth was retarded with 2 mg kg⁻¹ of depsipeptide at 7 days post-Pmel-1 CTL transfer. The acetylation level of histone H3 (lysine 18) also increased following depsipeptide treatment at target tumor sites (Figure 7b). Notably, this modulation was preferentially observed in the margin and perivascular area of the formed tumor (Figure S3a). A moderate induction

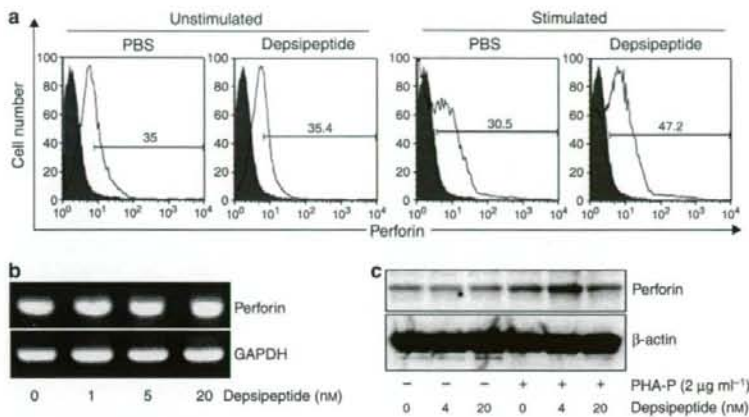


Figure 6. Effect of depsipeptide on perforin expression in effector T cells. (a) Increase of perforin-expressing antigen-stimulated pmel-1 T cells by exposure to depsipeptide (5 nM). Primary or antigen-stimulated Pmel-1 T cells (Thy1.1⁺) with or without depsipeptide (5 nM) for 16 hours were stained by FITC-conjugated anti-mouse perforin mAb after treatment with a Fixation & Permeabilization Kit (eBioscience). Shaded area represents isotype-matched control staining. (b) Antigen-stimulated Pmel-1 T cells were treated with depsipeptide at various concentrations for 16 hours, and then perforin mRNA was analyzed by RT-PCR (glyceraldehyde-3-phosphate dehydrogenase (GAPDH), an internal control). (c) Human CD8⁺ T cells were purified from peripheral blood mononuclear cells of healthy volunteers by magnetic bead selection and stimulated with or without PHA-P (2 μg ml⁻¹) *in vitro* for 24 hours. Cells were then lysed and probed for perforin and actin (as an internal control) by western blotting.

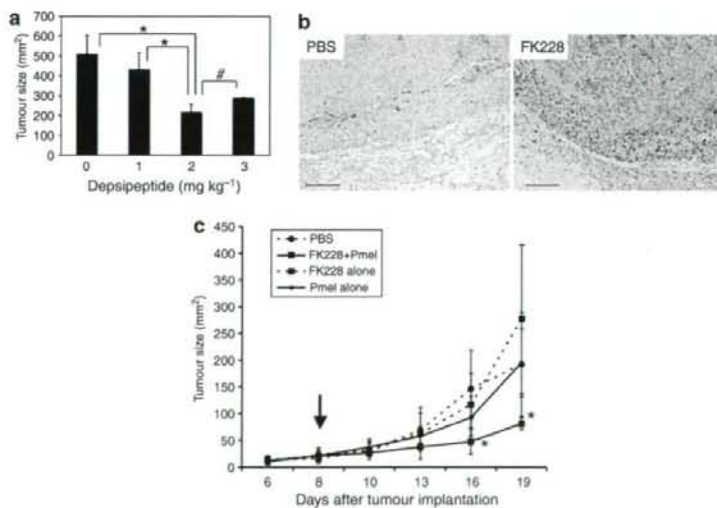


Figure 7. A limited dose of depsipeptide enhances CTL-mediated Luc-B16/F10 cell killing *in vivo*. (a) Effect of depsipeptide on B16/F10 tumor growth *in vivo*. B16/F10 cells (1×10^5) were inoculated subcutaneously into the abdominal skin of mice (day 0). A visible tumor in each mouse was established at day 7 after tumor implantation (average size: 122 ± 20 mm²), and mice were randomized and divided into four groups before treatment. Depsipeptide was administered intraperitoneally into mice from days 7–9 (only for 3 days) at the indicated dose, and activated Pmel-T cells (4×10^6) were subsequently injected intravenously into the tail vein of mice. Tumor growth was measured at day 21 after tumor implantation. The error bars represent the mean \pm SD ($n = 4$). * $P < 0.05$; [#] $P > 0.3$ (Mann-Whitney *U*-test). (b) Effect of depsipeptide on histone deacetylation in a subcutaneous tumor of B16/F10 cells. Established B16/F10 skin tumors 1 day after the final depsipeptide administration (2 mg kg⁻¹) were probed for acetyl-histone H3 (Lys 18) by immunohistochemistry (Bar = 100 μm). (c) Depsipeptide enhances CTL-mediated B16/F10 tumor killing *in vivo*. B16/F10 cells (5×10^5) were inoculated subcutaneously into the abdominal skin of mice (day 0). A visible tumor in each mouse was established at day 5 after tumor implantation. Depsipeptide (2 mg kg⁻¹) was administered intraperitoneally into mice from days 6–8 (for 3 days), and Pmel-1 CTLs (4×10^6) were subsequently injected intravenously into the tail vein of mice (indicated by the arrow). Tumor growth was monitored every 2–3 days after tumor implantation. The error bars represent the mean \pm SD ($n = 5–6$). * $P < 0.05$ (Kruskal-Wallis test; at days 16 and 19 after tumor implantation). One of three independent experiments with similar results is shown.

of gp100/pmel17 was also observed by RT-PCR assay (Figure S3b). Thus, these data demonstrate that a limited dose of depsipeptide (2 mg kg^{-1}) sufficiently sensitized B16/F10 cells *in vivo* for adoptive immunotherapy. Regarding the perforin modulation, we could not determine whether perforin induction occurred *in vivo* by FACS analysis.

We further investigated whether s.c. tumor growth of B16/F10 cells could be inhibited by the adoptive transfer of Pmel-1 CTLs in combination with depsipeptide (Figure 7c). After waiting about a week for tumor growth, 2 mg kg^{-1} of depsipeptide was administered via the intra-peritoneal route, followed by the adoptive transfer of Pmel-1 CTLs. In contrast to either CTL transfer alone or depsipeptide pretreatment alone, this combinatorial treatment strikingly suppressed B16/F10 tumor growth. Moreover, we examined whether the above depsipeptide pretreatment and a similar CTL transfer could suppress metastatic tumor growth (Figure 8). Luc-B16/F10 cells were intravenously injected into the tail vein of C57BL/6 mice, and pulmonary metastasis of luc-B16/F10 cells was monitored through luciferase-based luminescent imaging. After waiting about a week for tumor growth, animals were treated with 2 mg kg^{-1} of depsipeptide for 3 days, followed by the adoptive transfer of CTLs, which were generated by immunization using irradiated IL-12/IL-18-transduced B16/F10 cells. This combinatorial treatment significantly suppressed tumor-derived photons in pulmonary metastases 21 days following tumor injection. Similar suppression of pulmonary metastases was obtained by adoptive transfer of Pmel-1-derived CTLs (data not shown). Thus, these results demonstrate that sensitization using a limited dose of depsipeptide increases the efficacy of adoptive immunotherapy for established tumors.

DISCUSSION

Cellular unresponsiveness of solid tumor through aberrant transcriptional regulation represents a critical barrier that limits the therapeutic potential of adoptively transferred

autologous CTLs in patients with cancer. Herein, we have demonstrated that tumor sensitization with depsipeptide is effective for adoptive immunotherapy against murine B16/F10 melanoma. The remarkable features presented in this study include the following: (1) depsipeptide upregulated gp100/pmel17 melanoma antigen; (2) a limited dose of depsipeptide was able to sufficiently sensitize B16/F10 cells for Fas-mediated apoptosis; (3) depsipeptide increased the perforin-expressing CTLs in post-transcriptional levels; and (4) adoptive cell transfer in combination with depsipeptide led to effective tumor growth suppression.

Emerging evidence suggests that there are a variety of factors that limit tumor regression in the host-tumor interaction. For example, cancer progression often takes place despite the presence of circulating cancer-specific CTLs. Even with patients in whom large numbers of highly activated tumor-specific CTLs have been infused, clinical improvement has been difficult to achieve (Dudley *et al.*, 2001; Rosenberg, 2004). For example, recent evidence concerning host factors suggests that regulatory elements of the immune responses, including $\text{CD4}^+\text{CD25}^+$ regulatory T cells (Tregs), inhibit the ability of CTLs to produce effective antitumor responses (Antony and Restifo, 2005; Dannull *et al.*, 2005). In regard to tumor-escape factors, many aggressive tumors do not express the tumor antigen or MHC (HLA) antigen (Ferrone and Marincola, 1995; Cabrera *et al.*, 2003). Moreover, many cancer types lack sufficient apoptotic cell death pathways through the aberrant transcription (Johnstone *et al.*, 2002; Maecker *et al.*, 2002). It is theoretically essential to overcome these tumor-escape factors for efficient cancer immunotherapy, and perhaps to manipulate the tumor, as well as the host, before adoptive immune cell transfer.

HDACs are considered among the most promising targets in drug development for cancer, and some HDACi, including depsipeptide (FK228), are currently being tested in phase I and II clinical trials (Minucci and Pelicci, 2006). HDACi is capable of inducing varying degrees of growth arrest,

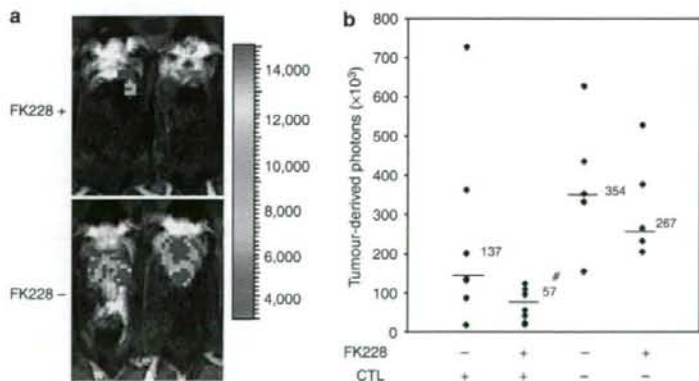


Figure 8. Depsipeptide pretreatment and B16-specific CTLs transfer suppress metastatic tumor growth of B16/F10 cells. (a) Representative luciferase images of luc-B16/F10 metastatic lung tumor at day 15 after combinatorial therapy of depsipeptide (2 mg kg^{-1}) and immune cell adoptive transfer from immunized mice using irradiated IL-12/IL-18-transduced B16/F10 cells. (b) Photon counting of luc-B16/F10-pulmonary metastasis at day 21 ($n=6-7$). $^*P<0.01$ (Kruskal-Wallis test). One of three independent experiments with similar results is shown.

differentiation, or apoptosis of cancer cells (Johnstone *et al.*, 2002; Minucci and Pelicci, 2006). In addition, normal fibroblasts and melanocytes are almost always considerably more resistant than tumor cells to depsipeptide (Kobayashi *et al.*, 2006; Minucci and Pelicci, 2006), suggesting this effect may be specific to malignant cells. We demonstrated the potential upregulation of MHC class I molecules by depsipeptide treatment. As the MHC class I molecule is released from the endoplasmic reticulum only after the peptide has bound and is allowed to reach the cell surface (Williams *et al.*, 2002), this upregulation could provide substantial benefits for the immunological recognition. However, there are abnormalities in the expression and/or function of various components of the MHC class I antigen-processing pathway in human malignant cells (Seliger *et al.*, 2000; Chang and Ferrone, 2007), and it remains to be elucidated whether HDACi affects various components of the protein-processing machinery.

Although the clinical use of depsipeptide when administered alone showed partial and complete responses in patients with hematological malignancy (Piekarz *et al.*, 2001, 2004; Byrd *et al.*, 2005), only a partially objective response was observed in solid cancer patients (Sandor *et al.*, 2002; Stadler *et al.*, 2006), suggesting that depsipeptide alone appears far from beneficial in the treatment of cancer patients. However, moving the focus onto the modulation of tumor factors and targeting HDACs could provide great benefits, particularly for selective immunotherapy against cancer. Intriguingly, HDACi could activate components of death receptor pathways, including FasL and tumor necrosis factor-related apoptosis-inducing ligand (TRAIL) (Nakata *et al.*, 2004; Singh *et al.*, 2005; Earel *et al.*, 2006). In fact, B16/F10 cells are less immunogenic and highly resistant to a variety of apoptotic stimuli if they are not manipulated (Avent *et al.*, 1979; Tsai *et al.*, 1997; Kalechman *et al.*, 1998). Nonetheless, exposure of B16 cells to a limited dose of depsipeptide induced cell surface expression of Fas and MHC class I, and the enforced Fas-engagement synergistically increased caspase-3/7 activity of B16/F10 cells in the presence of depsipeptide (Figure 3). Furthermore, these changes successfully provided CTLs with an enhanced ability to recognize and destroy target tumor cells (Figures 4 and 5).

Indeed, it has been demonstrated that HDACi synergizes with exogenously added TRAIL to induce apoptosis of various human solid tumor cell lines *in vitro* (Inoue *et al.*, 2004; Nakata *et al.*, 2004; Singh *et al.*, 2005; Lundqvist *et al.*, 2006). While the TRAIL system seems to be relatively major in the effect of HDACi on the human death receptor pathway, it has been suggested that the effect of HDACi on the death receptor pathway may not be universal (Minucci and Pelicci, 2006). We could not obtain a synergistic effect of depsipeptide with FasL in Fas-negative human MM-LH cells, and mouse Pmel-1 T cells did not express TRAIL on the cell surface (unpublished data). The Fas-FasL system is well known as the major pathway of CTL-mediated tumor destruction in murine models (Kagi *et al.*, 1994; Caldwell *et al.*, 2003; Lee *et al.*, 2006), and therefore some differences between species should be considered for the major death receptor pathway. However, current animal studies have

demonstrated that the augmented tumoricidal effects of tumor-specific CTLs induced as a consequence of depsipeptide sensitization resulted in melanoma cells that produced CTL-mediated cytotoxicity *in vivo*. A limited administration of depsipeptide also sufficiently modulated the acetylation level of histone H3 at the tumor site (Figure 7b). These findings may provide the rationale for protocols that pretreat cancer patients with depsipeptide to potentiate adoptive immune therapy.

Emerging experimental data indicate that lymphodepletion using cyclophosphamide before adoptive transfer of tumor-specific T lymphocytes plays a key role in enhancing treatment efficacy by eliminating regulatory T cells and competing elements of the immune system (Ghiringhelli *et al.*, 2004; Lutsiak *et al.*, 2005). Furthermore, pretreatment with cyclophosphamide contributes to the elimination of immunosuppressive cells such as CD4⁺CD25⁺ Treg in patients with cancer and the depletion of endogenous cells that compete for the activation of cytokines (known as the "cytokine sink") to maximize the exposure of homeostatic cytokines to the transferred CTLs (Gattinoni *et al.*, 2006). In addition to this pretreatment, depsipeptide may safely be added to reduce barrier tumor factors limiting the therapeutic potential of adoptively transferred CTLs. We further demonstrated that depsipeptide increased the level of perforin in activated T cells to varying degrees: the number of perforin-expressing CTLs increased in mice, whereas an accumulation of perforin was observed in humans. Perforin release by T cells in conjunction with granzymes induces an apoptotic cascade in target cells (Kagi *et al.*, 1994). In fact, Palmer *et al.* (2004) showed that there was a B16 cell-dependent release of perforin after adoptive cell transfer of pmel-1 T cells, in which caspase-3 activation was also shown at the tumor site as a consequence of the downstream activation of perforin. Therefore, the residual depsipeptide in the plasma of pretreated hosts could be expected to release large amounts of toxic granules to the target tumor at the sites and, in combination with cyclophosphamide, the use of depsipeptide may be considered for host and tumor modulation before adoptive tumor-specific CTL transfer.

The therapeutic options for patients with metastatic disease remain limited, and the majority of these patients will develop a local or systemic recurrence. A variety of human cancers such as melanoma and breast, colon, and prostate cancers aberrantly express the chemokine receptor CXCR4 (Balkwill, 2004; Kakinuma and Hwang, 2006; Zlotnik, 2006), and its activation through prosurvival pathways such as Akt has been implicated as a mechanism by which cancer cells evade host immunity (Murakami *et al.*, 2003) and increase their metastatic properties (Kakinuma and Hwang, 2006). Recently, Lee *et al.* (2006) reported that sensitization of B16 cells with a CXCR4 antagonistic peptide increases the efficacy of immunotherapy for pulmonary metastases, suggesting that the inhibition of tumor factor is an effective strategy for melanoma immunotherapy. Herein, we also provide compelling *in vitro* and *in vivo* data suggesting that sensitization of less immunogenic B16 cells with depsipeptide facilitates the efficacy of immunotherapy

for established pulmonary metastases. Further investigations based on the findings of this study, especially those incorporating *in vivo* techniques, should improve the design of optimized clinical protocols.

MATERIALS AND METHODS

Animals, cells, and reagents

Male C57BL/6 mice (8–12 weeks old) were purchased from Charles River Japan Inc. (Tsukuba, Japan). Pmel-1 TCR pmel-1 + Thy1.1 + transgenic mice (Overwijk et al., 2003) were obtained from The Jackson Laboratory (Bar Harbor, ME). All experiments in this study were approved by the animal ethics review board of Jichi Medical University and performed in accordance with the Jichi Medical University Guide for Laboratory Animals, following the principles of laboratory animal care formulated by the National Society for Medical Research.

Human melanoma cell lines RPM-MC, MM-LH, MM-BP, and MM-RU were kindly provided by Dr. H. Randolph Byers (Boston University Medical School) and maintained in minimal essential medium supplemented with 10% heat-inactivated fetal calf serum (FCS) (Byers et al., 1991). Murine B16/F10 melanoma cells (Fidler, 1973) and EL-4 thymoma cells (Ralph, 1973) were grown in DMEM (GIBCO, Gaithersburg, MD) with 10% FCS and supplements (Sato et al., 2006). Luciferase-expressing B16/F10 (luc-B16/F10) cells were generated previously (Sato et al., 2006) and maintained in DMEM with 10% FCS and supplements, including puromycin ($10 \mu\text{g ml}^{-1}$; Sigma-Aldrich, St Louis, MO). Normal human epidermal melanocytes were purchased from Kurabo Biomedicals (Osaka, Japan) and maintained in Medium 154S with supplement (Kobayashi et al., 2006). The cultures were kept in a humidified atmosphere containing 5% CO₂ and 95% air at 37°C.

Anti-acetyl-histone H3 (Lys 9), anti-acetyl-histone H3 (Lys 18), anti-histone H3, and anti-phospho-Rb (Ser 780) antibodies were purchased from Cell Signaling Technology (Beverly, MA). Anti-mouse p21^{Waf1/Cip1} (BD Pharmingen, San Diego, CA), anti-human perforin (clone 8G9; BD Pharmingen), and anti-actin (sc-16116, Santa Cruz Biotechnology Inc., Santa Cruz, CA) antibodies were used for western blotting. Flow cytometric analysis involved the use of phycoerythrin (PE)-conjugated anti-mouse H-2D^b mAb, PE-conjugated anti-mouse Fas (CD95) mAb, PE-conjugated anti-mouse FasL (CD178) mAb, and isotype-matched IgG controls, all of which were purchased from BD Pharmingen. FITC-conjugated anti-mouse perforin mAb (clone: eBioOMAK-D) was purchased from eBioscience (San Diego, CA). Anti-mouse FasL mAb (clone MFL3; BD Pharmingen) was used for the FasL neutralization.

The expression plasmids for mouse IL-12 and IL-18, pCAGGS-IL-12 and pCDNA-mproIL-18-mICE respectively, have been described previously (Ajiki et al., 2003). Depsipeptide (FK228) was obtained from Gloucester Pharmaceuticals (Cambridge, MA).

Reverse transcription-PCR

Total RNA was extracted from cells using Isogen (Nippon Gene, Toyama, Japan). Two micrograms of total RNA was used for first-strand synthesis using SuperScript III reverse transcriptase (Invitrogen, Carlsbad, CA). PCR was then performed using ExTaq polymerase (Takara, Ohtsu, Japan). The following primers were used for gp100/pmel-17 and perforin expression analysis: human gp100/pmel-17 sense, 5'-CCTCCTTCTCTATTGCCCTG-3'; human gp100/

pmel-17 anti-sense, 5'-TGTAGGAGAGGTGAGCTTCA-3'; mouse gp100 sense, 5'-GGCCAACAACACCATCATCA-3'; mouse gp100 anti-sense, 5'-GGGCAAGATGAGAGGATGA-3'; mouse perforin sense, 5'-ACAATAACAATCCCCGGTGG-3'; mouse perforin anti-sense, 5'-TGGGATTAAGCGCTGTGCT-3'; glyceraldehyde-3-phosphate dehydrogenase sense, 5'-GTATCGTGAAGGACTCATG-3'; and glyceraldehyde-3-phosphate dehydrogenase anti-sense, 5'-AGTGGGTGTCGGCTGTTGAAG-3'. PCR conditions for each set of primers included an initial treatment at 95°C for 2 minutes, followed by 30 cycles consisting of denaturation at 95°C for 15 seconds, annealing at 57°C for 30 seconds, and then extension at 72°C for 2 minutes. PCR products were analyzed using a 1% agarose gel.

Transfection and ELISA

B16/F10 cells (1×10^6) were transfected with pCAGGS-IL-12 (5 μg) and pCDNA-mproIL-18-mICE (5 μg) using Lipofectamine 2000 (Invitrogen). Immunization experiments involved irradiating IL-12/IL-18-transfected B16 cells with 80 Gy 36 hours after transfection. Irradiated cells ($1-2 \times 10^5$) were then injected twice into the subcutaneous space of C57BL/6 mice during the remaining weeks.

To analyze IFN- γ production, splenocytes ($1-2 \times 10^5$) that were isolated from immunized mice were co-cultured for 24 hours with 1×10^5 irradiated target cells, and the IFN- γ concentration of supernatants was then measured using a mouse IFN- γ immunoassay kit. All samples were assayed in triplicate.

Apoptosis and cytotoxic assay

To detect caspase-3/7 activity, B16/F10 cells (2×10^4 per well of a 96-well plate) were plated, and the Caspase-Glo 3/7 Assay system (Promega, Madison, WI) was used for analysis in accordance with the manufacturer's instructions 16 hours after the addition of depsipeptide. The background luminescence associated with the cell culture and assay reagent (blank reaction) was subtracted from experimental values. Means of triplicates were used to represent caspase-3/7 activity for the given cells. Each experiment was performed three times with similar results.

For enhancement of Fas-mediated apoptosis, B16/F10 cells were exposed to 10 ng ml^{-1} recombinant human FLAG-tagged FasL (Apotech, San Diego, CA) in combination with 1 mg ml^{-1} anti-FLAG M2 mAb (Sigma, St Louis, MO) for 16 hours with 5 nM depsipeptide at 37°C in the presence of 0.5% FCS, as described previously (Murakami et al., 2003). After exposure of B16/F10 cells to apoptosis-enhancing conditions for 16 hours, attached (and detached) cells were collected from tissue culture plates for annexin-V staining according to the manufacturer's instructions (MEBCYTO Apoptosis Kit; MBL, Nagoya, Japan). Analysis of caspase-3/7 activity involved the assessment of 2×10^4 cells using the Caspase-Glo 3/7 Assay system (Promega).

Western blotting and flow cytometry

For western blotting, cells were lysed by sonication in radio-immuno-protein assay (RIPA) buffer (Sato et al., 2006) and then centrifuged for 10 minutes at 4°C. Each cell extract (10 μg of protein) was assayed using appropriate antibodies and protein G-conjugated horseradish peroxidase (Amersham Pharmacia Biotech, Buckinghamshire, UK).

For the flow cytometric analysis, cells (1×10^6) were washed with phosphate buffered saline (PBS) and incubated with mAb for

30 minutes at 4°C. Following washing with 0.1% FCS-PBS, cells were analyzed using FACS Calibur (Becton Dickinson, Mountain View, CA) and FlowJo analysis software (Tree Star, San Carlos, CA).

Subcutaneous and intravenous tumor inoculation

Cells in an exponential growth phase were harvested by trypsinization and washed twice in PBS before injection. For the s.c. injections, cells (1×10^6) were injected into the abdominal subcutaneous space of C57BL/6 mice. Tumor growth at the skin was monitored by measurement of the two maximum perpendicular tumor diameters. For the intravenous injections to the lungs, luc-B16/F10 cells (5×10^4 in 0.2 ml PBS) were injected into the tail vein of C57BL/6 mice. Each experiment was performed 2–4 times with similar results.

In vivo bioluminescence imaging

In vivo tumor progression was examined using the noninvasive bioimaging system IVIS (Xenogen, Alameda, CA). Tumor-implanted mice were anesthetized with a mixture of ketamine and xylazine, and D-luciferin (potassium salt; Biosynth, Postfach, Switzerland) was injected into the peritoneal cavity at 2 mg per animal, which was followed immediately by the measurement of luciferase activity. The imaging system consisted of a cooled, back-thinned charge-coupled device camera to capture both a visible light photograph of the animal taken with light-emitting diodes and a luminescent image. After acquiring photographic images of each mouse, luminescent images were acquired with a 1–15 minutes exposure time (Ohsawa et al., 2006; Sato et al., 2006). Images were obtained with a 25 cm field of view, a binning (resolution) factor of 8, 1/f stop, and an open filter. The resulting gray scale photographic and pseudo-color luminescent images were automatically superimposed by software to facilitate the identification of any optical signal and the location on the mouse. Optical images were displayed and analyzed using Igor (WaveMetrics, Lake Oswego, OR) and IVIS Living Image (Xenogen) software packages. The signal from tumors was quantified as photons flux in units of photons per second per cm² per sr.

Immunohistochemistry

Removed specimens were fixed with 10% paraformaldehyde and embedded in paraffin. Tissue sections (5 µm) deparaffinized in xylene were passed through graded alcohols before being treated with 1% H₂O₂ (v/v) in H₂O for 20 minutes at room temperature. After washing the sections three times with PBS, sections were blocked for 20 minutes with 10% FCS diluted in PBS. All incubations were performed at room temperature in a moist chamber. The slides were incubated overnight at 4°C with anti-acetyl-histone H3 (Lys 18) antibody (no. 9675, Cell Signaling Technology) diluted 1:100 in blocking solution. The sections were washed in PBS and incubated with biotinylated goat anti-rabbit secondary antibody (Vector Laboratories, Burlingame, CA), and staining was visualized using a streptavidin-peroxidase conjugate (Vector Laboratories). A diaminobenzidine substrate kit (Vector Laboratories) was used for color (brown) visualization, and sections were counterstained with hematoxylin.

Statistical analysis

P-values based on two-sided Student's *t*-test, Mann-Whitney test, or Kruskal-Wallis test were obtained using the Instat software package

(GraphPad, San Diego, CA). Differences between groups were considered significant if $P < 0.05$.

CONFLICT OF INTEREST

The authors state no conflict of interest.

ACKNOWLEDGMENTS

We would like to thank Ms Yasuko Sakuma, Ms Yumi Ohde, and Ms Masayo Kumagai for their skillful technical assistance. This study was supported by a grant to T.M. from the Kowa Life Science Foundation (2004) and the Ministry of Education, Culture, Sports, Science and Technology (MEXT) of Japan (Project No. 17591181; 2005–2007) and by a grant from the "High-Tech Research Center" Project for Private Universities: matching fund subsidy from MEXT (2003–2007).

SUPPLEMENTARY MATERIAL

Figure S1. Expression of HLA class I (A, B, C) and Fas (CD95/Apo-1) in human melanoma cell lines following exposure to depsipeptide.

Figure S2. Increase of perforin in PHA-stimulated human T cells by exposure to depsipeptide (4 nM).

Figure S3. Effect of depsipeptide on the subcutaneous tumor of B16/F10 cells.

REFERENCES

- Ajiki T, Murakami T, Kobayashi Y, Hakamata Y, Wang J, Inoue S et al. (2003) Long-lasting gene expression by particle-mediated intramuscular transfection modified with bupivacaine: combinatorial gene therapy with IL-12 and IL-18 cDNA against rat sarcoma at a distant site. *Cancer Gene Ther* 10:318–29
- Antony PA, Restifo NP (2005) CD4+CD25+ T regulatory cells, immunotherapy of cancer, and interleukin-2. *J Immunother* 28:120–8
- Avent J, Vervaert C, Seigler HF (1979) Non-specific and specific active immunotherapy in a B16 murine melanoma system. *J Surg Oncol* 12: 87–96
- Balkwill F (2004) Cancer and the chemokine network. *Nat Rev Cancer* 4: 540–50
- Byers HR, Etoh T, Doherty JR, Sober AJ, Mihm MC Jr (1991) Cell migration and actin organization in cultured human primary, recurrent cutaneous and metastatic melanoma. Time-lapse and image analysis. *Am J Pathol* 139:423–35
- Byrd JC, Marcucci G, Parthun MR, Xiao JJ, Klisovic RB, Moran M et al. (2005) A phase I and pharmacodynamic study of depsipeptide (FK228) in chronic lymphocytic leukemia and acute myeloid leukemia. *Blood* 105:959–67
- Cabrera T, Lopez-Nevot MA, Gaforio JJ, Ruiz-Cabello F, Garrido F (2003) Analysis of HLA expression in human tumor tissues. *Cancer Immunol Immunother* 52:1–9
- Caldwell SA, Ryan MH, McDuffie E, Abrams SI (2003) The Fas/Fas ligand pathway is important for optimal tumor regression in a mouse model of CTL adoptive immunotherapy of experimental CMS4 lung metastases. *J Immunol* 171:2402–12
- Chang CC, Ferrone S (2007) Immune selective pressure and HLA class I antigen defects in malignant lesions. *Cancer Immunol Immunother* 56: 227–36
- Dannull J, Su Z, Rizzieri D, Yang BK, Coleman D, Yancey D et al. (2005) Enhancement of vaccine-mediated antitumor immunity in cancer patients after depletion of regulatory T cells. *J Clin Invest* 115: 3623–33
- Dudley ME, Wunderlich J, Nishimura MI, Yu D, Yang JC, Topalian SL et al. (2001) Adoptive transfer of cloned melanoma-reactive T lymphocytes for the treatment of patients with metastatic melanoma. *J Immunother* 24:363–73
- Earell JK Jr, VanOosten RL, Griffith TS (2006) Histone deacetylase inhibitors modulate the sensitivity of tumor necrosis factor-related apoptosis-inducing ligand-resistant bladder tumor cells. *Cancer Res* 66: 499–507

- Ferrone S, Marincola FM (1995) Loss of HLA class I antigens by melanoma cells: molecular mechanisms, functional significance and clinical relevance. *Immunol Today* 16:487-94
- Fidler IJ (1973) Selection of successive tumour lines for metastasis. *Nat New Biol* 242:148-9
- Gattinoni L, Powell DJ Jr, Rosenberg SA, Restifo NP (2006) Adoptive immunotherapy for cancer: building on success. *Nat Rev Immunol* 6:383-93
- Chiringhelli F, Larmonier N, Schmitt E, Parcellier A, Cathelin D, Garrido C et al. (2004) CD4⁺CD25⁺ regulatory T cells suppress tumor immunity but are sensitive to cyclophosphamide which allows immunotherapy of established tumors to be curative. *Eur J Immunol* 34:336-44
- Herman JC, Baylin SB (2003) Gene silencing in cancer in association with promoter hypermethylation. *N Engl J Med* 349:2042-54
- Hoshikawa Y, Kwon HJ, Yoshida M, Horinouchi S, Beppu T (1994) Trichostatin A induces morphological changes and gelsolin expression by inhibiting histone deacetylase in human carcinoma cell lines. *Exp Cell Res* 214:189-97
- Inoue S, MacFarlane M, Harper N, Wheat LM, Dyer MJ, Cohen GM (2004) Histone deacetylase inhibitors potentiate TNF-related apoptosis-inducing ligand (TRAIL)-induced apoptosis in lymphoid malignancies. *Cell Death Differ* 11(Suppl 2):S193-206
- Johnstone RW, Licht JD (2003) Histone deacetylase inhibitors in cancer therapy: is transcription the primary target? *Cancer Cell* 4:13-8
- Johnstone RW, Ruefli AA, Lowe SW (2002) Apoptosis: a link between cancer genetics and chemotherapy. *Cell* 108:153-64
- Kagi D, Vignaux F, Ledermann B, Burki K, Depraetere V, Nagata S et al. (1994) Fas and perforin pathways as major mechanisms of T cell-mediated cytotoxicity. *Science* 265:528-30
- Kakinuma T, Hwang ST (2006) Chemokines, chemokine receptors, and cancer metastasis. *J Leukoc Biol* 79:639-51
- Kalechman Y, Strassmann G, Albeck M, Sredni B (1998) Up-regulation by ammonium trichloro(dioxoethylene-0,0') tellurate (AS101) of Fas/Apo-1 expression on B16 melanoma cells: implications for the antitumor effects of AS101. *J Immunol* 161:3536-42
- Klisovic DD, Katz SE, Efron D, Klisovic MI, Wickham J, Parthun MR et al. (2003) Depsipeptide (FR901228) inhibits proliferation and induces apoptosis in primary and metastatic human uveal melanoma cell lines. *Invest Ophthalmol Vis Sci* 44:2390-8
- Kobayashi Y, Ohtsuki M, Murakami T, Kobayashi T, Sutesophon K, Kitayama H et al. (2006) Histone deacetylase inhibitor FK228 suppresses the Ras-MAP kinase signaling pathway by upregulating Rap1 and induces apoptosis in malignant melanoma. *Oncogene* 25:512-24
- Lee CH, Kakinuma T, Wang J, Zhang H, Palmer DC, Restifo NP et al. (2006) Sensitization of B16 tumor cells with a CXCR4 antagonist increases the efficacy of immunotherapy for established lung metastases. *Mol Cancer Ther* 5:2592-9
- Lundqvist A, Abrams SI, Schrumph DS, Alvarez G, Suffredini D, Berg M et al. (2006) Bortezomib and depsipeptide sensitize tumors to tumor necrosis factor-related apoptosis-inducing ligand: a novel method to potentiate natural killer cell tumor cytotoxicity. *Cancer Res* 66:7317-25
- Lutsiak ME, Semnani RT, De Pascalis R, Kashmiri SV, Schlom J, Sabzevari H (2005) Inhibition of CD4(+)/25(+) T regulatory cell function implicated in enhanced immune response by low-dose cyclophosphamide. *Blood* 105:2862-8
- Maecker HL, Yun Z, Maecker HT, Giaccia AJ (2002) Epigenetic changes in tumor Fas levels determine immune escape and response to therapy. *Cancer Cell* 2:139-48
- Marks P, Rifkin RA, Richon VM, Breslow R, Miller T, Kelly WK (2001) Histone deacetylases and cancer: causes and therapies. *Nat Rev Cancer* 1:194-202
- Minucci S, Pellicci PG (2006) Histone deacetylase inhibitors and the promise of epigenetic (and more) treatments for cancer. *Nat Rev Cancer* 6:38-51
- Murakami T, Cardones AR, Finkelstein SE, Restifo NP, Klaunberg BA, Nestle FO et al. (2003) Immune evasion by murine melanoma mediated through CC chemokine receptor-10. *J Exp Med* 198:1337-47
- Nakata S, Yoshida T, Horinaka M, Shiraishi T, Wakada M, Sakai T (2004) Histone deacetylase inhibitors upregulate death receptor 5/TRAIL-R2 and sensitize apoptosis induced by TRAIL/APO2-L in human malignant tumor cells. *Oncogene* 23:6261-71
- Ohsawa I, Murakami T, Uemoto S, Kobayashi E (2006) *In vivo* luminescent imaging of cyclosporin A-mediated cancer progression in rats. *Transplantation* 81:1558-67
- Overwijk WW, Theoret MR, Finkelstein SE, Surman DR, de Jong LA, Vyth-Dreese FA et al. (2003) Tumor regression and autoimmunity after reversal of a functionally tolerant state of self-reactive CD8⁺ T cells. *J Exp Med* 198:569-80
- Palmer DC, Balasubramaniam S, Hanada K, Wrzesinski C, Yu Z, Farid S et al. (2004) Vaccine-stimulated, adoptively transferred CD8⁺ T cells traffic indiscriminately and ubiquitously while mediating specific tumor destruction. *J Immunol* 173:7209-16
- Piekarz RL, Robey R, Sandor V, Bakke S, Wilson WH, Dahmouh L et al. (2001) Inhibitor of histone deacetylation, depsipeptide (FR901228), in the treatment of peripheral and cutaneous T-cell lymphoma: a case report. *Blood* 98:2865-8
- Piekarz RL, Robey RW, Zhan Z, Kayastha G, Sayah A, Abdeldaim AH et al. (2004) T-cell lymphoma as a model for the use of histone deacetylase inhibitors in cancer therapy: impact of depsipeptide on molecular markers, therapeutic targets, and mechanisms of resistance. *Blood* 103:4636-43
- Ralph P (1973) Retention of lymphocyte characteristics by myelomas and theta-lymphomas: sensitivity to cortisol and phytohemagglutinin. *J Immunol* 110:1470-5
- Rosenberg SA (2004) Shedding light on immunotherapy for cancer. *N Engl J Med* 350:1461-3
- Rosenberg SA, Dudley ME (2004) Cancer regression in patients with metastatic melanoma after the transfer of autologous antitumor lymphocytes. *Proc Natl Acad Sci USA* 101(Suppl 2):14639-45
- Rosenberg SA, Yang JC, Restifo NP (2004) Cancer immunotherapy: moving beyond current vaccines. *Nat Med* 10:909-15
- Sandor V, Bakke S, Robey RW, Kang MH, Blagosklonny MV, Bender J et al. (2002) Phase I trial of the histone deacetylase inhibitor, depsipeptide (FR901228, NSC 630176), in patients with refractory neoplasms. *Clin Cancer Res* 8:718-28
- Sato A, Ohtsuki M, Hata M, Kobayashi E, Murakami T (2006) Antitumor activity of IFN- λ in murine tumor models. *J Immunol* 176:7686-94
- Seliger B, Maeurer MJ, Ferrone S (2000) Antigen-processing machinery breakdown and tumor growth. *Immunol Today* 21:455-64
- Singh TR, Shankar S, Srivastava RK (2005) HDAC inhibitors enhance the apoptosis-inducing potential of TRAIL in breast carcinoma. *Oncogene* 24:4609-23
- Stadler WM, Margolin K, Ferber S, McCulloch W, Thompson JA (2006) A phase II study of depsipeptide in refractory metastatic renal cell cancer. *Clin Genitourin Cancer* 5:57-60
- Tsai V, Southwood S, Sidney J, Sakaguchi K, Kawakami Y, Appella E et al. (1997) Identification of subdominant CTL epitopes of the GP100 melanoma-associated tumor antigen by primary *in vitro* immunization with peptide-pulsed dendritic cells. *J Immunol* 158:1796-802
- Ueda H, Manda T, Matsumoto S, Mukumoto S, Nishigaki F, Kawamura I et al. (1994a) FR901228, a novel antitumor bicyclic depsipeptide produced by *Chromobacterium violaceum* No. 968. III. Antitumor activities on experimental tumors in mice. *J Antibiot (Tokyo)* 47:315-23
- Ueda H, Nakajima H, Hori Y, Goto T, Okuhara M (1994b) Action of FR901228, a novel antitumor bicyclic depsipeptide produced by *Chromobacterium violaceum* no. 968, on Ha-ras transformed NIH3T3 cells. *Biosci Biotechnol Biochem* 58:1579-83
- Williams A, Peh CA, Elliott T (2002) The cell biology of MHC class I antigen presentation. *Tissue Antigens* 59:3-17
- Zlotnik A (2006) Chemokines and cancer. *Int J Cancer* 119:2026-9

ラットを基盤とした *in vivo* バイオイメージング

村上 孝, 小林英司

われわれは、これまで医療技術を模倣できる動物資源に注目し、体サイズの大きいラットを用いた臓器移植研究を行ってきた。特に、移植された細胞系譜の運命を追跡するため、genetic marker probeを広範な組織に発現するトランスジェニック (Tg) ラットを作製してきた。数年の歳月をかけて構築した「color-engineered rat」システムでは、蛍光と発光の双方のレポーターシステムを利用することが可能であり、生体内における移植細胞の挙動について詳細な分析を行うことができる。本稿では、われわれが行ってきた「ラット」を基盤とした研究とそのイメージングの利用について概説する。

はじめに

ヒトゲノム情報を含む先端医学の成果は、マウスやラットなどのゲノム情報と比較され、それぞれ臓器固有の発生や分化機構の解明に大きく貢献している。

【キーワード&略語】

トランスジェニックラット、臓器移植、動物資源、生体内イメージング

CsA : cyclosporine A (シクロスポリンA)

CXCR4 : CXC chemokine receptor 4 (CXCケモカイン受容体4)

DSG : 15-deoxyspergualin (デオキシスパーガリン)

ES細胞 : embryonic stem cells

GFP : green fluorescent protein (緑色蛍光タンパク質)

Luc : luciferase (ルシフェラーゼ)

MSC : mesenchymal stem cell (間葉系幹細胞)

SDF-1 α : stromal-derived factor 1 alpha (ストローマ細胞由来因子1 α)

Tg : transgenic (トランスジェニック)

さらに、GFPの特徴や簡便な利用性をきっかけに、生きた細胞をリアルタイムに観察できるバイオプローブの開発や細胞や小動物を生きた状態で観察できるバイオイメージング技術が大きく進歩している。現代の医生物学研究では、機能分子の挙動が生きた細胞や実験動物個体内での生体内イメージング情報として捉えられようとしている。

われわれの研究の出発点は臓器移植^{※1}にあり、「移植された臓器や組織がどのような運命をたどるのか」、また「移植臓器の生着をいかに延長させることができるか」が焦点であった。心臓や肝臓などの実質臓器を安定して顕微鏡下手術 (マイクロサージェリー) によ

※1 臓器移植

移植片 (臓器・組織: ドナー) がレシビエント (移植を受ける側) に受け入れられるか否かは遺伝的な近縁度に左右される。「同種同系」では拒絶反応は起こらず、「同種異系」もしくは「異種」移植の際に拒絶反応が生じる。免疫学的な拒絶反応の程度は主要組織適合性複合 (major histocompatibility complex : MHC) 抗原の差異に依存する。

in vivo bio-imaging using the rat

Takashi Murakami/Eiji Kobayashi : Division of Organ Replacement Research, Center for Molecular Medicine, Jichi Medical University (自治医科大学分子病態治療研究センター臓器置換研究部)

表 color-engineered rat

ラットの系統	プロモーター	マーカー
Wistar	CAGGS ^{a)}	GFP ^{b)}
Lewis	CAGGS	GFP
Lewis	Albumin	GFP
Dark Agouty	CAGGS	LacZ (β -ガラクトシダーゼ)
Lewis	ROSA26	LacZ (β -ガラクトシダーゼ)
Wistar	Albumin	DsRed2 ^{c)}
Wistar	CAGGS	DsRed2, GFP (Cre/loxPシステム)
Lewis	ROSA26	ルシフェラーゼ ^{d)}
Lewis	ROSA26	DsRed単量体

a) cytomegalovirus enhancer/chicken β -actin promoter, b) green fluorescent protein (*Aequorea victoria*), c) DsRed (*Discosoma*), d) luciferase from the firefly (*Photinus pyralis*)

り移植できる実験動物のサイズは「ラット」にある¹⁾。ラットは、マウスと比べて体サイズが10倍も大きいいため、特定部位へのカテーテル挿入など、臨床医学で利用される種々の技術を応用することができる。われわれは、実際の医療応用への視点から「医療技術を模倣できる動物資源」に注目し、移植・再生医療のためのモデル動物開発を行ってきた。本稿では、われわれがこれまで行ってきた蛍光・発光ラットのモデルとバイオイメージングを用いた研究の例を紹介したい。

1 蛍光タンパク質を発現する トランスジェニックラット・システム

実験動物としての歴史では、マウスよりもラットの方が早く医学研究に応用されてきた背景があり、特に薬理学や脳神経科学の分野におけるラットの実験データは現在の臨床医学・薬学研究の礎となっている¹⁾。ラットにトランスジェニック技術が応用されたのはマウスに遅れること約10年、1990年代ははじめになる^{2) 3)}。これまでトランスジェニック (Tg) ラットの作製では、受精卵膜がマウスのものに比べて脆弱なため、その作製効率が悪いとされていた。しかし、高度なマイクロインジェクション技術が安定して行われるようになり、現在では高率に遺伝子導入個体を得ることができるようになっている。発現されるcDNAの性質に依存するものの、1匹のTgラットを得るためには少なくとも100個の受精卵にマイクロインジェクションする必要がある。また、広範な組織に発現可能

なプロモーターを有するベクターが用いられても、組込まれた染色体の位置やコピー数などの要素によって、発現する臓器や発現量も異なる性質がある。したがって、広い用途でのTgラットのライン化は必ずしも容易ではない。

生きた細胞を励起光下で観察できるGFPは、細胞動態観察のみならず細胞内タンパク質の挙動を観察する「biological light probe」として現代のバイオサイエンスを支える重要なアイテムになっている⁴⁾。赤橙色や青色などの蛍光タンパク質との組み合わせにより、細胞機能を「色分け」することができる。傷害を受けた組織の機能的回復を目指す再生医学研究では、移植した細胞や組織の運命を追跡する研究は応用的な医療技術への方向性を決める重要な律速段階となる。したがって、細胞機能を「色分け」し、移植細胞が機能回復にどのように関与するか評価できるシステムはきわめて重要な意味をもつ。生体イメージング技術が著しく発展した結果、応用的なバイオ研究を目指す研究者にとっては、種々のバイオプローブをもつトランスジェニックラットの利用価値は高く、移植された細胞や組織の動態を「光」として追跡することが可能である。臓器移植研究への必要性からはじまった「color-engineered rat」(表)の開発も進み、9種類が再生医学を含むさまざまな研究分野に利用されている。

われわれの作製したCAG/GFP-LEW Tgラットは中枢神経系などで輝度が強く、神経前駆細胞を用いた

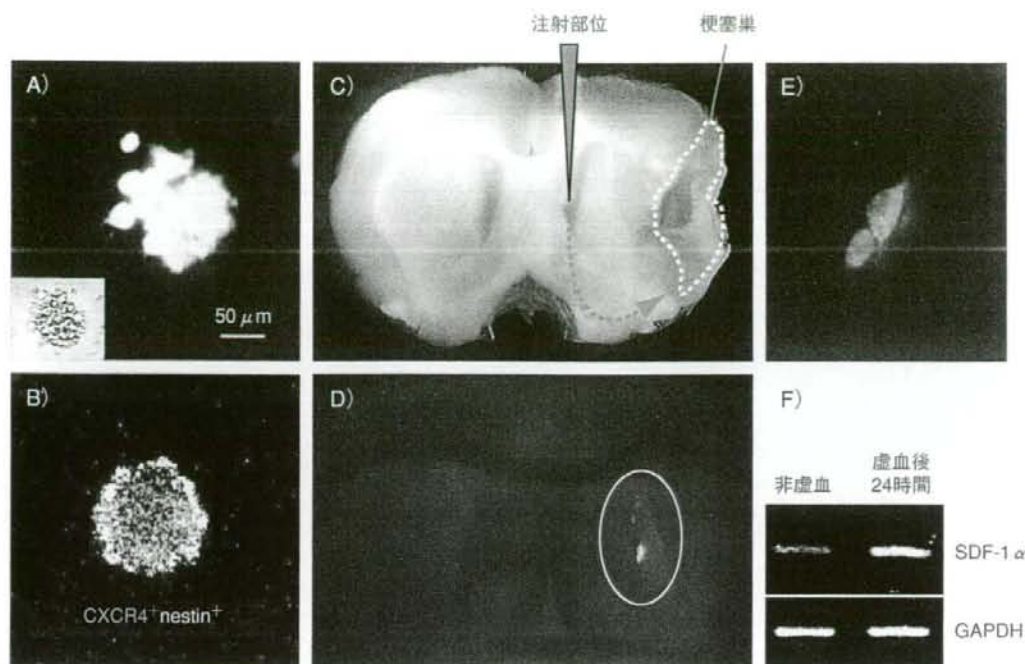


図1 GFP-Tgラットを用いた神経前駆細胞の動態

A) CAG/GFP-LEW Tgラット (胎生14.5日) から分離・作製した神経前駆細胞集塊 (20日間培養), 489nmの励起光下でGFPの蛍光が観察される。B) 神経前駆細胞集塊におけるCXCR4 (赤) とnestin (緑) の発現。C) ラットに実験的脳梗塞を作製し, 5日後にGFP+神経前駆細胞を定位脳手術的に脳室内に注入した際の模式図。D) C標本を489nmの励起光下での観察。梗塞部位にGFP+神経前駆細胞が集積 (注入後28日目)。E) Dの拡大画像。F) 梗塞部位 (24時間後) におけるSDF-1 α のRT-PCR解析。CXCR4のリガンドであるSDF-1 α の発現が増加 (文献1, 5より転載)

再生医学研究に応用されている^{5)~7)}。例えば, 胎生14.5日から作製した神経前駆細胞は, 脳質内に投与すると実験的脳梗塞部位に集積する性質がある (図1)。この主な細胞集積にはケモカイン受容体であるCXCR4やスフィンゴシン1-リン酸 (sphingosin-1-phosphate: S1P) 受容体の関与を示唆する結果が得られている^{1)~3)}。これらの受容体は7回膜貫通G-タンパク質結合型受容体として, 走化性, 細胞運動, 細胞接着などを活性化することができる。

また, われわれは肝特異的にDsRed2 (赤橙色) を発現するラット⁹⁾やCre/loxP (DsRed2/GFP) Tgラットなども開発している¹⁰⁾。アルブミンプロモーターで作動するAlb-DsRed2 Tgラットから骨髓細胞を採取し, 肝傷害を加えたラットに門脈投与すると, 骨髓細胞が傷害肝内でアルブミン産生細胞に変化している様子が観察される (図2A~C)。また, Cre/loxP

(DsRed2/GFP) ダブルレポーターラットでは, 下肢移植による筋肉の融合により, GFPの発現が観察することができる (図2D~G)。しかし, このような蛍光タンパク質を用いた個体内での細胞・組織動態が観察できるようになるまでには, 特定の生物現象が時間的に決定されている必要がある。

2 ダブルTgラット作製とその応用

前述の蛍光タンパク質の検出には励起光源を必要とするが, 発光タンパク質の「光」を指標に評価する系がある。例えば, ホタル由来のルシフェラーゼは, 高感度で組織透過性と定量性に優れた光 (フォトン) を発生し, 目的とする細胞や組織における遺伝子発現をリアルタイムに追跡することを可能にする。生体を透過する最適な光 (600nm) が得られるルミネセンス法は検出感度と定量性の点で非常に有利である。この発